V. CRYOGENIC AND SUPERCONDUCTING MAGNETS

James C. Laurence, Gerald V. Brown, Willard D. Coles, and Gale Fair

The Lewis Research Center has primary NASA responsibility for research on advanced concepts of power generation and propulsion. Some of these concepts require intense, large-volume, magnetic fields to be generated by lightweight equipment with low power consumption. Electric propulsion, magnetohydrodynamic power generation, thermonuclear power and propulsion, and space radiation shielding are some concepts for which such magnetic fields may be required.

The development of intense magnetic fields is also of importance for studies in a variety of disciplines, such as elementary particle physics (e.g., accelerators and bubble chambers), solid-state physics, and plasma physics. The range of size and field which are available in existing electromagnets is illustrated in figure V-1. The largest volume magnets are the bubble chamber magnets of Argonne National Laboratory, Brookhaven National Laboratory, and the French national laboratory at Saclay, which range in size to about 6 meters at 2 to 3 teslas. To put the measurement of magnetic flux density in perspective, the Earth's magnetic field is approximately 10^{-4} tesla (or 1 G) and a strong permanent magnet may range up to 1 tesla. The magnets described herein vary from 1 to a planned 30 teslas.

The work of Bitter and others at the Massachusetts Institute of Technology (MIT) resulted in a funding by the U.S. Air Force of a national magnet laboratory which is now known as the Francis Bitter National Magnet Laboratory. It has the largest concentration of high-field magnets in the world and is the center for research in intense fields. Their water-cooled copper solenoids reach flux densities of 22.5 teslas in a 3- to 4-centimeter bore, and 26.5 teslas in a very small volume with iron pole pieces.

The Lewis neon-cooled aluminum electromagnets have produced 20 teslas in a 11.5-centimeter-diameter volume and 14 teslas in a 30-centimeter-diameter volume. Lewis also has a 15-tesla superconducting magnet with a 16-centimeter-diameter bore (the largest and strongest superconducting magnet yet produced). Both MIT and McGill University are working on hybrid magnets - MIT on a superconducting magnet with a water-cooled insert, and McGill on a superconducting magnet with a cryocooled aluminum insert.

When the program to provide large-volume, intense magnetic fields was initia-

ted at Lewis, several different means of producing these fields were investigated. To reduce structural problems and simplify magnet construction and operation, it was decided to use low-impedance, high-current design. This design criterion was applied first to copper water-cooled coils, and later to aluminum cryogenically cooled coils.

A large homopolar generator (fig. V-2) and a transformer-rectifier power supply (fig. V-3) were selected as the power sources for the low-impedance electromagnets. The homopolar machine, a direct-current generator, supplies 3 megawatts power and a maximum of 200 000 amperes. The rectified alternating-current supply furnishes 1 megawatt with a maximum of 28 000 amperes.

The low-impedance concept has the following advantages:

(1) The magnet windings can be made in large cross sections to take advantage of the very heavy currents that can be drawn from the machine. These conductors are inherently stronger because of their size and may be nearly self-supporting in the fields produced.

(2) Since the potential difference between turns of a magnet designed according to this concept is small (of the order of a few volts), no special high-voltage insulation or water treatment is necessary. The cooling water can be drawn from the mains and disposed of in the sewer. In addition, there are no hazards because of high voltage.

(3) Cryogenic cooling of the conductors, which reduces their resistance by a factor of 1000 or more, can be used in the design of the magnets.

Two water-cooled magnets (one of which is shown in figs. V-4 and V-5, have been designed and built to operate from the homopolar generator. The magnet shown has a 10-centimeter bore and can reach 8.8 teslas.

It is hard to get high-current density, structural strength, and low-power consumption simultaneously in magnet windings. It is still harder to use the conductor material itself as the structure. The massive turns of the water-cooled magnets are self-supporting; but, at much higher current densities, pure copper is not strong enough to support itself. Some copper alloys (e.g., BeCu and ZrCu) have much higher strength with only moderately increased resistivity. However, still greater gains in strength and much lower resistivity are possible with specialization. Many steels have better elastic properties than the copper alloys and are better for structural support. On the other hand, some high-purity metals cooled to cryogenic temperatures have resistivities of only one-hundredth to one-thousandth that of copper at room temperature. Thus it is desirable to separate the functions of conduction and stress support. Greater strength and lower power consumption result. These are the principal advantages of cryogenically cooled (nonsuperconductive) electromagnets.

CRYOGENIC MAGNETS

Conductors and Coolants

The advantage of the cryogenically cooled but nonsuperconducting magnet systems comes from the low resistance of the conductor. Commercial copper, for example, has a resistance at the boiling point of helium that is one-hundredth its resistance at room temperature. The resistance ratio of a material, the ratio of the room-temperature resistance to the resistance at 4.2 K, is the working measure of the purity of the material. The temperature dependence of the resistivity for some pure metals with resistance ratios of about 1000 is shown in figure V-6. From this figure, it can be seen that the temperature range of importance is below 20 to 30 K. Commercial aluminum can be produced with a resistance ratio of 2000, and the temperature dependence of its resistivity is similar to that of copper shown in figure V-6.

Another significant factor in cryogenic magnet design is the magnetoresistance of the conductor, At these low temperatures, the resistance of a pure metal depends on the magnetic field. For example, in figure V-7, the data for the resistivity of copper to 11.5 teslas show a linear dependence on magnetic field strength. Figure V-8 shows data for aluminum taken at two temperatures. The aluminum magnetoresistance saturates at a low field, making this aluminum a strong candidate for high-field, cryogenically cooled electromagnets.

Below 30 K, the only coolant fluids are neon, hydrogen, and helium. Liquid helium, at 4.2 K, is not a good coolant for pool-boiling heat transfer because the latent heat of vaporization is so small. The hazards of liquid hydrogen preclude its use in a populated area such as the Lewis Research Center. The choice then was to use liquid neon at 27 K.

The only known source of the inert gas neon is the Earth's atmosphere, where it occurs at a concentration of about 18 ppm. Since neon is inert, there are no safety problems except those inherent with any cryogenic liquid. Large-scale production of oxygen for the steel industry during the last decade has made neon available in large supply at a considerable reduction in cost. Even so, the cost of operating with liquid neon is about $40 per liter, which is prohibitive unless the gas is recovered and reliquefied for reuse. The capital investment for the Lewis neon liquefier was one-third that of a cold-helium gas system large enough to cool the magnets. In addition, liquid neon is a desirable cryogen for a boiling-heat-transfer application because of its large latent heat per unit volume. Hence, liquid neon was chosen as the coolant for the Lewis cryogenic electromagnets.

The commercial high-purity aluminum, with about 17 ppm impurities and a re-

sistance ratio of 2000, was chosen as the conductor material for two magnets with inner diameters of 11.5 and 30 centimeters. Figure V-9 is a cutaway drawing of the completed 30-centimeter aluminum cryomagnet and its containment vessel. The construction of the cryostat is illustrated, including the vacuum jacket, the liquid-nitrogen jacket, and the trace lines for precooling of the magnet vessel and coils.

Aluminum Magnet Construction

The construction of the aluminum coils is shown in figure V-10. Each turn of the magnet is a composite structure providing the current path, structural strength, coolant passages, and insulation. The high-purity aluminum conductor is 5 centimeters wide by 0.2 centimeter thick. It was anodized to produce a uniform coating of aluminum oxide on the surface. This coating serves to insulate the aluminum from the stainless-steel channel and to improve the boiling heat transfer by providing additional sites for incipient boiling. The stainless-steel channel supports the very soft, annealed aluminum on three sides and also provides the hoop strength and much of the turn-to-turn and coil-to-coil bearing surface. Flow channels for the liquid-neon coolant are provided by stainless-steel spacer bars held in place by a thin corrugated carrier ribbon of stainless steel. A glass and epoxy resin cloth provides insulation between turns.

Two bore sizes of this magnet have been built and have been in service for about 5 years. The magnet coils are electrically connected in a series-parallel arrangement to work within the voltage and current ranges of the homopolar generator.

A completed stack of these coils ready to be inserted in the cryostat is shown in figure V-11. Clearly shown in this figure are the bus bars and the intercoil connections. These must not only carry the current, but must resist the forces developed by the interaction of the current and the field.

The real usefulness of these magnets is determined by their operating characteristics. Some of the operating characteristics of the 20-tesla magnet are presented in figure V-12, which shows the change in resistance of the coils over the operating range. The change in resistance as the magnet is energized is caused by the change in magnetoresistance of the aluminum conductor as the field increases and by the heating of the conductor as the current increases. Because the liquid neon is boiling under saturated conditions into a fixed-volume vapor recovery tank, the temperature of the liquid rises some 3° as the pressure in the system increases. This results in higher resistance values as the current is returned toward zero.

The operation of the liquid-neon-cooled magnets is limited by the capacity of the

refrigeration system, which is approximately 80 liters of liquid neon per hour. This limitation can be better expressed as one period of operation per day. The duration of a period of operation depends on the field strength desired. At maximum field (i.e., maximum power consumption), the time of operation is about 1 minute, including time to run up to field, time of operation at desired field strength, and time to shut down. The time is much longer, of course, for lower field ranges (about 4 min at 10 T). During a typical day's operation, one field sweep to 18 teslas and one to 16 teslas have been achieved. The power required for the maximum field (20 T) is 1 megawatt at 33 volts and 15 000 amperes in each of two parallel sets of coils (30 000 A total). The stored energy is approximately 10 megajoules. The total power consumed by the aluminum magnet is one-twentieth of the power required for water-cooled magnets of the same field strength and volume of field.

Some other advantages of the cryogenically cooled magnets are

(1) The fields can be swept quite rapidly, and for many experiments this is ideal.

(2) Ripple and noise fields are very small ($\approx 10^{-3}$ T).

(3) The general design is appropriate for solenoids of still higher field strength, higher than those possible with superconducting magnets made with presently known superconducting materials.

The major disadvantages of cryogenically cooled magnets are the short operating time at maximum field, the large capital investment for the refrigeration plant, and the large magnet coils and cryostats. Despite these disadvantages, the magnets are reliable and produce high-intensity fields for research in basic physics and in engineering applications.

What place do cryogenic magnets have in the future now that superconducting magnets, which require no power, are a reality? Recent work concerns methods of extending the field range of these magnets.

Future Potential

Clearly, the future of cryogenic magnets will be in areas where superconducting magnets cannot function or are uneconomical. The most obvious regime where cryomagnets will be important is in fields too strong for superconductors. Above 15 teslas at present and above perhaps 20 teslas in the foreseeable future, superconductors cannot carry useful amounts of current. Thus it may always remain true that cryogenic magnets will be used to reach fields higher than those possible with the best superconductors. A planned improvement in the aluminum cryomagnet at Lewis should allow fields between 25 and 30 teslas to be reached for laboratory

research in solid-state physics and for engineering studies on materials to be used in high fields. Another area of some current interest is alternating-current or pulsed applications where the superconductors do exhibit resistance. Here the power expended in a high-purity cryogenic coil may be lower than in a superconducting coil. Furthermore, in other conditions where energy is dissipated in the magnet windings, such as by electromagnetic radiation and neutrons from a thermonuclear reaction, it may be necessary to operate the coil hotter than attainable critical temperatures of superconductors to reduce refrigeration power.

Current Study Areas

At Lewis, engineering analysis is being directed at the very-high-field cryomagnet, with 30 teslas as the nominal design goal. This is twice the highest field so far attained with superconductors, and 7.5 teslas higher than the strongest steady field yet attained.

The crux of the engineering problem at this field level is the competition for space in the magnet windings between the three principal factors - current density, strength, and cooling. A fourth factor, insulation, is essential but usually not a problem. A 30-tesla solenoid must have a current density of the order of 5 to 10 kiloamperes per square centimeter to have reasonably compact windings. At these current densities, the force on a 1-foot length of 1-inch-square conductor in a 30-tesla field is between 40 and 80 tons. The I^2R power dissipated in this volume is likely to exceed 100 watts for the purest available aluminum at helium temperature and 5 to 10 times as much for operation in hydrogen or neon. These power densities are very low compared to typical values in water-cooled magnets, but nevertheless pose moderate to severe problems for cryogenic coolants, which have relatively smaller heat capacities and latent heats. Finally, the extreme softness and low yield strength make plastic flow of very pure aluminum a definite problem because of the extremely large forces. These three problems - magnet mechanical strength, adequate cooling, and conductor softness - are paramount in the cryogenic magnet engineering problem.

The 30-tesla coil under design and study here at Lewis poses a very severe cooling problem. Figure V-13 contrasts the conductors of the existing cryomagnet and of the proposed 30-tesla insert coil. The cooling in the existing coil depends on natural convection of the liquid neon in the rather large cooling channels. In the new design (called "second generation"), the coolant is pumped through smaller channels to achieve much higher heat fluxes and thus to allow higher current densities. Less space is wasted in the new design because the material between cooling chan-

nels is aluminum, which can carry current, rather than steel filler or spacer bars. The purity of the aluminum to be used is not so high that its softness will cause any great problem. At the temperature of liquid neon, an increase in the purity of the aluminum does not offer much resistivity advantage over moderate purity.

Ultra-high-purity aluminum has recently been made commercially feasible for a magnet construction material. The advantage of this material is the lower residual resistance, but to take full advantage of the low resistance of this ultra-high-purity aluminum, the operating temperature must be dropped to 10 K or below. Thus, the only possible coolant is helium, either as a liquid or as a supercritical fluid. The solutions of the strength, cooling, and plastic-flow problems for this situation are different enough to merit the classification of such high-purity coils as "third-generation" cryogenic magnets. As yet no such third-generation coil is under detailed mechanical design. But, a preliminary look has been taken at the main features that such a coil might have.

First the conductor should be a thin, wide ribbon, backed up by a ribbon of steel or other strong material, as shown in figure V-14. The forces on the thin-ribbon conductor can thus be passed to the structure through a large bearing area, and large strains and plastic flow are thereby avoided. The grooved conductor design of the second-generation coils would be carried over. These interleaved ribbons of conductor and steel (and a suitable thin film of insulation) would be wound into the common "pancake" or "tape-wound" coil. The figure shows several thin ribbons of steel. Several thin ribbons are preferred to a single thick one so that the number of ribbons can vary from the inside of the coil to the outside. Variations in strength requirements from inside to outside make this desirable. In fact, analysis shows that if the total thickness of the bundle of steel ribbons varies in the appropriate way, the turn-to-turn forces that would pass through the soft aluminum can be reduced almost to zero. At the same time, a troublesome problem inherent in tape-wound coils, the tendency of the coils to loosen and unwind when energized, can be avoided. This unwinding is due to the outer turns of the coil stretching more than the inner ones. A numerical solution of an integral equation is required to find the proper variation of steel thickness. Figure V-15 shows one such result for a 30-tesla coil. The solid curve shows the desired variation in steel thickness as a function of radius. The dashed lines show how this calculated variation could be approximated by adding more thin steel ribbons as the coil is wound to give the greater rigidity needed in the outer turns.

Figure V-16 shows how a 20-tesla coil wound with these techniques would compare in winding size and in power requirement with the existing first-generation 20-tesla coil for the same inner diameter and length. Winding volume is only one-sixteenth as much and the required power only one twenty-fifth as much. The

superiority of the third-generation design is even more pronounced at still higher fields.

This is the direction of the present work at Lewis on cryogenic magnets. However, it is anticipated that most space applications will use superconducting magnets.

SUPERCONDUCTING MAGNETS

The phenomenon of superconductivity in metals was first observed in the early 1900's. It is characterized by a total loss of resistance to electrical current in a step transition as temperature is reduced to near absolute zero. Since the first studies of the phenomenon, nearly all metals have been categorized as either superconducting or ferromagnetic at very low temperatures. Most of the metals revert to their normal resistance characteristics in relatively low magnetic field environments that are externally applied or self-generated by a current flow in the metal, or when their temperature exceeds a characteristic low critical temperature. These critical values are not mutually independent but are rather the extreme values of a bounding surface between the superconducting and normal states, as indicated in figure V-17. For values of current, magnetic field strength, and temperature less than critical, the material is superconducting. For values greater than these critical values (i.e., for points outside the critical surface), the materials are normal (resistive) conductors. A characteristic of these materials is the Meissner effect illustrated in figures V-18 and V-19. Figure V-18 shows a normal conductor, such as copper, where the flux lines completely penetrate the sample. Also shown is a superconductor which excludes the flux completely (e.g., tin). This phenomenon is characteristic of superconductors classified as type I. The type II superconductors are illustrated in figure V-19. The behavior is similar to that of type I superconductors in low fields, but at high fields the flux penetrates partially into the conductor and produces normal and superconducting regions.

Type I superconductors are further characterized by low values of critical temperature, while the type II materials have the highest known critical temperatures. In the type I materials, the flux enters the conductor at the critical field or critical temperature, and the conductor reverts to the resistive state. In type II materials, however, the flux enters in discrete packets with a gradual change to the normal state. It was not until 1961, with the discovery of materials capable of retaining their superconducting characteristics at high field strengths (over 20 T) and relatively high temperatures (to 20 K) and while carrying high current densi-

ties (over 10^6 A/cm^2), that significant commercial use of superconductors could be made.

Current-against-field curves are indicative of the maximum current that a short sample of a type II superconductor can carry as a function of the applied magnetic field. These curves for three of the most commonly used superconducting materials are shown in figure V-20. The niobium-tin compound Nb_3Sn is an intermetallic compound with the highest critical temperature T_c and critical magnetic field strengh H_c of the practical materials (18.5 K and 22 T). Niobium titanium (Nb-Ti) is an alloy with an H_c somewhat greater than 11 T. This alloy has displaced Nb-Zr, an earlier development, in practical applications.

Figure V-21 shows the current density that can be carried by Nb_3Sn produced by three different methods. Large variations like these are possible because current-carrying ability is determined by the number and nature of imperfections in the material. Magnetic flux penetrates high-field superconductors in individual tubes enclosed in a vortex of current, as shown in figure V-22. These so-called "flux lines" or vortices generate heat if they move through the superconductor, and may, in fact, drive the superconductor back into its normal state. It is thus necessary for the flux lines to be immobilized by blocking them with imperfections in the superconductor. These imperfections are called pinning sites. Dislocations, voids, and precipitates are among those imperfections known to be effective pinning sites. The more numerous and effective the pinning sites are, the more current the superconductor can carry. Unfortunately, during the charging period of a coil, the flux must move to some degree, and the resulting heating can decrease the effectiveness of the pinning sites, allowing more motion and more heating at an increasing rate. This magnetic and thermal runaway, called a flux jump, can drive a small part of the superconductor back into the normal state. This normal region may expand and cause the quench of the entire coil. A reliable method of preventing the spread of a normal region is to provide sufficient copper in parallel with the superconductor. The effect of the copper is to shunt the current around the normal region temporarily to allow the normal region to cool and become superconducting again. This composite conductor is known as a "stabilized conductor" and was first demonstrated by Kantrowitz and Stekly in 1965. The added copper gives stability at the considerable expense of a reduction in current density. Efforts to obtain stabilization with higher current density are discussed later in the section Stabilized Superconductors.

The Lewis Research Center has acquired a number of superconducting magnets with a large range of size and field strength, as shown in figure V-23. The solid circles represent Lewis superconducting magnets, and the solid squares the Lewis cryocooled magnets. The superconducting magnets with the largest bore diameters

are those built for a plasma physics facility, the Superconducting Magnetic Mirror Apparatus (SUMMA). The coils are 51 centimeters in inside diameter and have 4.5-tesla fields. Dr. Roth's plasma physics apparatus, the first built with superconducting magnets is also represented in figure V-23. It has an inside diameter of 18 centimeters and a 2.5-tesla field. Also shown are magnets used in solid-state physics research, as well as the 16-centimeter, 15-tesla magnet. The open circles denote the Argonne National Laboratory (ANL) and Brookhaven National Laboratory (BNL) bubble chamber magnets, while the diamonds denote the Bitter National Magnet Laboratory (NML) water-cooled magnets.

The cryostats for the Lewis magnets vary in size from a few liters to over 1400 liters liquid-helium capacity. Boiloff gas from the larger facilities is collected, and reliquefied in a system (fig. V-24) consisting of two hemispherical balloons 27.5 meters in diameter, a purification system, and two 100-liter-per-hour liquefiers. This liquid-helium system was originally acquired for, and is mostly used by, a space environment simulation facility.

The upper section of the largest magnet cryostat is shown in figure V-25. It has an inside diameter of almost 1 meter and is 4.2 meters in height, most of which is below floor level.

Some of the smaller magnets compared in figure V-23 are similar to those used at other laboratories, so the remaining discussion is concerned with those that are unique to Lewis.

The highest field attained anywhere thus far with superconducting magnets is about 15 teslas, which was attained with the 15-centimeter-bore magnet at Lewis. This magnet has a test volume approximately nine times that of the other highest-field superconducting magnets.

Lewis 15-Centimeter-Bore, 15-Tesla Magnet

Design and construction of the 15-tesla magnet presented some problems which, though not unique, were intensified by the size and field strength requirements. The magnet and Dewar lid assembly is shown in figure V-26. The magnet is a solenoid with approximate dimensions of 15 centimeters in inside diameter, 50 centimeters in outside diameter, and 35 centimeters in length. Weight of the magnet is nearly 1000 pounds, and the stored energy when powered to maximum field strength approaches 2 megajoules.

At present, Nb_3Sn is the only commercially available superconducting material which is suitable for use in a magnetic environment greater than about 10 teslas. The 90 000 meters of 1/4-centimeter-wide superconductive ribbon used in the mag-

net is a composite of Nb_3Sn, stainless steel, and silver. Stainless steel serves as a base for the vapor-deposited Nb_3Sn and provides the high strength required. Silver plating is added to improve the stability of the superconductor. The thickness of each material is varied as a function of the characteristics required. Excess thickness of any of the materials is costly in terms of current density, and as a result is costly in magnet volume, materials, and performance.

Matching of the conductor to the field, strength, and stability requirements in different sections of the magnet led immediately to a modular design concept. Hoop stress on the conductor and compressive loading of the magnet windings and internal structure are necessarily high because of the high current densities required. Axial compressive loading of the windings builds up throughout the magnet as a result of the attractive force between conductors. To prevent compressive stress from exceeding the strength limits of the materials, load-bearing radial and axial members were required. The module walls serve this purpose, accepting and transmitting forces at various points in the magnet. A computer program was used to optimize the design, both as to strength and conductor characteristics. Figure V-27 shows various parts of the magnet. Twenty-two coil forms were used to wind the 30 electrically distinct modules.

Because of the large mass of the magnet, cooling of the internal parts was essential. Grooves and holes in the support structure provide passages for the inflow of liquid helium and for the escape of helium gas. No provision is made for helium passages within the windings. Heat is generated by localized "flux jump" penetrations or general transitions from superconductive to resistive modes. These transitions result in the collapse of the field and the release of all of the stored energy in a very short time period. When this occurs, the magnet is heated, and the helium is vaporized.

Superconducting Magnetic Mirror Magnets

A set of 51-centimeter-bore magnets in an axial array is to be used in a superconducting magnetic mirror apparatus. Four of the six 51-centimeter magnets are quite similar in construction and materials to the 15-centimeter magnet. These magnets, shown in figure V-28, are not made from stabilized material, although one does use a copper-clad conductor. As a result, all these magnets are readily triggered into the superconducting-to-normal transition, or quench, and none achieved design current or field strength goals in their initial tests. However, by operating the magnets in superfluid helium, design values were, for the most part, obtained. Magnet performance was improved by factors of from 1.3 to 1.6 over

the performance obtained when 4.2 K helium was used.

Superfluid helium occurs as an increasing fraction of liquid helium as the temperature is reduced below 2.17 K. The characteristics of the superfluid are no less amazing than those of a superconductor, and indeed there are theoretical analogies between the two. The two characteristics of the superfluid which make it unique as a coolant are its extremely high thermal conductivity and extremely low viscosity. Within certain limits of heat flux, all the heat generated anywhere in the liquid is conducted essentially instantaneously to the surface of the liquid. When this behavior is combined with what is, for all practical purposes, zero viscosity, there results a coolant that literally searches for heat, penetrating even the smallest opening. This results in improved superconductor stability and allows the attainment of higher current values.

The remaining two 51-centimeter-bore magnets, not previously discussed, are shown in figure V-29 shortly after removal from the Dewar following a test. They are each 80 centimeters in outside diameter and 30 centimeters long. Weight of the magnet pair is over 2 tons. The magnets are made in three concentric modules, and are wound of stabilized NbTi and Nb_3Sn.

The two types of conductor used are illustrated in figure V-30. The innermost module, shown during assembly (fig. V-31), consists of 20 submodules of 1.25-centimeter-wide Nb_3Sn ribbon stabilized with copper and strengthened with stainless steel. An intermittent insulation of mylar is used. This conductor is wound in pancake form. Outer modules (fig. V-32) are spool-wound using a 0.218-centimeter-square composite of copper and NbTi. Since this set of magnets is wound of stabilized materials, little additional performance benefit can be realized by operation of these magnets in superfluid helium.

Stabilized Superconductors

The superconducting coils of today represent great advances over their normal predecessors. But they are not yet satisfactory for space applications. Whereas reliable, compact coils to reach high fields are needed, at present a choice must be made between compactness and reliability. The quest for compactness is really a quest for higher current density.

At present, the standard method of preventing thermal runaway is to place copper in parallel with the superconductor, as previously mentioned. But the amount of copper needed is several times the amount of superconductor, which makes the winding several times as large and massive. This is undesirable for aerospace magnets. The most obvious improvement is to use pure aluminum, which has much

higher electrical conductivity under magnet conditions than copper. The resulting composite conductor may look something like that shown in cross section in figure V-33(a). A substrate of steel for strength is first coated with superconductor on both sides and then clad with aluminum. The amount of aluminum needed could be very small, as pictured. The size of the same type of composite using copper is shown for comparison in figure V-33(b).

Bonding aluminum to other metals is difficult, but fortunately, a bond may not be necessary. If the aluminum is close enough to the superconductor for good magnetic coupling, induced eddy currents can prevent flux from moving too fast. The rate of heat generation is thus brought under control, and stability is achieved. At present, this appears to be the most promising and efficient stabilization method suitable for use with Nb_3Sn. Both experimental and analytical work is in progress here at Lewis and elsewhere on this use of aluminum.

The amount of aluminum needed and, hence, the attainable composite current density are rather difficult to calculate accurately, but the basic thinking goes like this. The flux must be restricted to move slowly enough that the heat generated in the superconductor can be conducted away without too much rise in temperature. Superconductors are such poor heat conductors that only very thin layers or very small diameter wires can be considered. Otherwise, the internal regions of the superconductor cannot be held below the critical temperature. For the layered geometry pictured in figure V-33, the required thickness of normal material varies as the cube of the superconductor thickness. This favors a thin superconductor. On the other hand, for a fixed thickness of substrate, the overall current density drops if the superconductor becomes very thin. Thus, for each substrate thickness, the right choice of superconductor and aluminum thicknesses gives the best current density. Figure V-34 shows the way in which the realizable overall current density depends on the basic substrate thickness. The upper envelope curve is obtained if forces can be neglected. The other curves are for various force-limited conditions where extra steel is needed for strength. If practical considerations allow thin substrates, superconductor layers, and aluminum layers, very good current densities can be achieved because the required amount of aluminum can be very small.

Advanced Superconductivity Concepts

In this section, some of the research areas in superconductivity that promise to have the greatest effect on magnet and propulsion technology are discussed briefly. Currently, the most extensive and fruitful research area is the development of new alloys and intermetallic compounds that have higher critical fields or

critical temperatures, or both. The materials mentioned herein, such as Nb_3Sn and NbTi, represent valuable products of this research. Because so little is known about the electronic properties of the many, many possible alloys and compounds, it is necessary to try different combinations by guesswork and intuition.

As an example of the effort involved in this area, consider the compound Nb_3Sn, which plays an important role in magnet technology. This is a compound of the transition metal niobium with the simple metal tin. The transition temperature for this compound is 18.5 K, still below the boiling point of hydrogen, and the critical field is about 22 teslas. For several years, this was the highest transition temperature known. Research into compounds of niobium with other simple metals has resulted in the recent discovery of the material $Nb_3 (Al_{1-X} Ge_X)$ with a transition temperature of about 20.7 K, a significant increase.

This research effort constitutes an attempt to understand the mechanism of superconductivity in metals and alloys of metals, within the framework of present knowledge about electronic properties of simple metals. The work discussed in the following paragraphs represents a search for a new mechanism for superconductivity, outside the realm of metals.

As a preface to this discussion of new mechanisms in superconductors, let us briefly review the mechanism of superconductivity in metals, at least as it is currently understood. Superconductivity arises from an attractive interaction between conduction electrons in a metal. Figure V-35 shows schematically how this interaction arises. An electron, with a negative charge, moves through the lattice of ion cores, displacing the ion cores from their normal positions. The result is a net positive charge in the region behind the passing electron. Another electron, following in the path of the first, feels a force due to this charge. The energy of this interaction between the electrons, and ultimately, the critical temperature of the superconductor, is determined by the speed with which the lattice can respond to these disturbances. This model for superconductivity is usually referred to as "the electron-phonon interaction."

The exciting new developments in superconductivity stem from attempts to find other mechanisms for an electron-electron interaction. The most interesting and controversial model has been proposed by Little, in the form of an organic superconductor. Figure V-36 shows, with artistic license, a model of a polymer chain with periodic side branches. Little's model for the interaction consists of an electron moving along the "spine" and causing a polarization of the charge in the side branches. In the same manner as in the electron-phonon interaction, this polarization causes a force on another electron moving along the spine. Little estimates that transition temperatures of the order of 10^3 K might be feasible for a suitable polymer. Thus far, no experimental evidence for an organic superconductor has

been found, although several investigations are in progress.

The final, and most promising, model is the so-called "excitonic superconductor." Figure V-37 shows a portion of the boundary between a metal and a dielectric. An electron initially in the dielectric may be excited and hence move into the metal, leaving a hole behind. This hole acts essentially as a positive charge, attracting an electron in a surface state within the metal and thus creating the same type of attractive interaction as occurred in the other models. The critical temperature for this system is determined by the energy necessary to excite the initial electron, and could correspond to hundreds of degrees. A practical manifestation of this model seems to be a layered structure, composed of alternating sheets of metal and insulator, possibly in the form of a ribbon. Such an excitonic superconductor, having a high transition temperature, would certainly cause a breakthrough in magnet design and other engineering applications.

One word of caution should be noted, however. Very little is known about the properties of electrons in these materials. For example, even if an excitonic superconductor should be discovered, the critical field and critical current characteristics of the material determine its application to technology. So little is known about the superconducting state in these materials that nothing may be said about these critical parameters. In spite of these uncertainties, there are hopes that one or another of these concepts may lead to a revolutionary development in magnet technology.

In summary, the goal of a lightweight, stable, high-field, large-volume electromagnet has not yet been reached. Indeed, the common practice has been to increase the weight and decrease the current density of the superconducting magnet by including a large amount of copper (or other nonsuperconductor) as a stabilizer in parallel with the superconductor. In some respects, this means that the magnet is essentially a cryogenically cooled nonsuperconducting magnet, at least during some phases of its operation.

But there are some promising developments which may reverse this trend. Composites of normal metals and very many fine filaments of the superconductor, twisted and superimposed, are becoming available. Dynamic stabilization with high-purity aluminum will be realized. The future holds (1) a continuing search for high-field, high-current, and high-critical-temperature alloys and compounds; (2) attempts to develop high-critical-temperature organic materials; and (3) attempts to enhance superconducting properties by thin-film, sandwiched conductors.

The most exciting possibilities for new applications of the results of the magnet research and development of the last 10 years are high-field magnets for direct conversion of energy by MHD and thermonuclear power generation; power transmission in underground superconducting or cryogenically cooled lines; and rotating machinery with field coils and/or armatures with superconducting windings.

BIBLIOGRAPHY

This bibliography comprises publications authored by the members of the NASA Lewis Research Center Staff.

Aron, P. R.; and Ahlgren, G. W.: Critical Surfaces for Commercial Nb_3Sn Ribbon and Nb-25% Zr Wire. Advances in Cryogenic Engineering. Vol. 13. K. D. Timmerhaus, ed., Plenum Press, 1968, pp. 21-29.

Aron, Paul R.; and Chandrasekhar, B. S.: Magnetostriction in Single-Crystal Bismuth. Bull. Am. Phys. Soc., vol. 10, no. 9, Nov. 1965, p. 1201.

Aron, Paul R.; and Chandrasekhar, B. S.: Oscillatory Magnetostriction and Deformation Potentials in Bismuth. Bull. Am. Phys. Soc. vol. 14, no. 3, Mar. 1969, p. 306.

Boom, R. W.; and Laurence, J. C.: Force-Reduced Superconducting Toroidal Magnet Coils. Presented at the NAS-NRC Cryogenic Engineering Conference, Los Angeles, Calif., June 16-18, 1969.

Brown, Gerald V.: The Excitation Spectrum for a Bose Gas with Repulsive and Attractive Interactions. NASA TN D-4838, 1968.

Brown, Gerald V.: High-Field Cryogenic Magnets with Pure Aluminum Conductor. Presented at the Symposium on Engineering Problems of Fusion Research, Los Alamos, N. Mex., Apr. 8-11, 1969.

Brown, G. V.; and Coles, W. D.: High-Field Liquid-Neon-Cooled Electromagnets. Advances in Cryogenic Engineering. Vol. 11. K. D. Timmerhaus, ed., Plenum Press, 1966, pp. 638-642.

Brown, Gerald V.; and Coopersmith, Michael H.: Excitation Spectrum for a Bose Gas with Repulsive Core and Attractive Well. Phys. Rev., vol. 178, no. 1, Feb. 5, 1969, pp. 327-344.

Brown, Gerald V.; and Flax, Lawrence: Superposition Calculation of Thick Solenoid Fields from Semi-Infinite Solenoid Tables. NASA TN D-2494, 1964.

Brown, Gerald V.; and Flax, Lawrence: Superposition of Semi-Infinite Solenoids for Calculating Magnetic Fields of Thick Solenoids. J. Appl. Phys., vol. 35, no. 6, June 1964, pp. 1764-1767.

Brown, Gerald V.; Flax, Lawrence; Itean, Eugene C.; and Laurence, James C.: Axial and Radial Magnetic Fields of Thick, Finite-Length Solenoids. NASA TR-170, 1963.

Callaghan, Edmund E.; and Maslen, Stephen H.: The Magnetic Field of a Finite Solenoid. NASA TN D-465, 1960.

Callaghan, Edmund E.; and Flax, Lawrence: Radial Flux or Field of an Isotropic, Cylindrical Source of Finite Extent. NASA TN D-873, 1961.

Callaghan, Edmund E.: Anisotropic Effects in Helically Wound Superconducting Solenoids. NASA TN D-2083, 1963.

Callaghan, Edmund E.: Potential Advantages of Anisotropic Superconductors in "Force-Free" Solenoids. NASA TN D-2156, 1964.

Callaghan, Edmund E.; and Stoll, James C.: Azimuthal Magnetic Field of a Thick, Finite-Length, Helical Solenoid. NASA TN D-2372, 1964.

Coles, Willard D.; Brown, Gerald V.; Meyn, Erwin H.; and Schrader, E. R.: Pumped Helium Tests of a 51-Centimeter Bore Niobium-Tin Magnet. NASA TN D-5158, 1969.

Coles, W. D.; Laurence, J. C.; and Brown, G. V.: Cryogenic and Superconducting Magnet Research at the NASA Lewis Research Center. Presented at AIChE Sixty-Second Annual Meeting, Washington, D.C., Nov. 16-20, 1969.

Coles, W. D.; Schrader, E. R.; and Thompson, P. A.: A 14-Tesla 15-Centimeter-Bore Superconductive Magnet. Advances in Cryogenic Engineering. Vol. 13. K. D. Timmerhaus, ed., Plenum Press, 1968, pp. 142-149.

Fair, Gale: Theory of Galvanomagnetic Effects in Metals. Ph.D. Thesis, Case Western Reserve Univ., 1969.

Fair, Gale; and Taylor, P. L.: Exact Semiclassical Theory for Galvanomagnetic Effects in Metals. NASA TN D-4166, 1966.

Fakan, John C.; and Schrader, Edward R.: Experimental Evidence of Degradation Effects in Short Samples of Hard Superconductors. NASA TN D-2345, 1964.

Flax, L.: Monotonic Magnetostriction for Diamagnetic Materials. Phys. Letters, vol. 19, no. 6, Dec. 1, 1965, pp. 469-471.

Flax, Lawrence: The Theory of the Anisotropic Heisenberg Ferromagnet. Ph.D. Thesis, Colorado State Univ., 1969.

Flax, Lawrence; and Callaghan, Edmund E.: Magnetic Field from a Finite Thin Cone by Use of Legendre Polynomials. NASA TN D-2400, 1964.

Flax, Lawrence; and Raich, John C.: Spin-Wave Approximation for an Anisotropic Heisenberg Model. Bull. Am. Phys. Soc., vol. 13, no. 6, June 1968, p. 903.

Flax, Lawrence; and Raich, John C.: Random Phase Approximation for the Anisotropic Heisenberg Ferromagnet. NASA TN D-5286, 1969.

Flood, Dennis J.: Magnetothermal Oscillations in Pressure-Annealed, Pyrolytic Graphite. NASA TN D-5488, 1969.

Flood, D. J.: Molecular Vibration Spectra from Field Emission Energy Distribution. Phys. Letters, vol. 29A, no. 2, Apr. 7, 1969, pp. 100-101.

Flood, D. J.: Magnetothermal Oscillations in Pressure-Annealed Pyrolytic Graphite. Phys. Letters, vol. 30A, no. 3, Oct. 6, 1969, pp. 178-179.

Hudson, Wayne R.: Effect of Tensile Stress on Current-Carrying Capacity of Commercial Superconductors. NASA TN D-3745, 1966.

Hudson, Wayne R.; Copper Magnetoresistance Devices as Magnetometers. NASA TN D-3536, 1966.

Hudson, W. R.: Negative Magnetoresistance in Carbon Resistance Thermometers. Rev. Sci. Instr., vol. 39, no. 2, Feb. 1968, pp. 253-254.

Hudson, Wayne R.; and Jirberg, Russell J.: Nonlinear Flux Flow in Single Crystal Niobium. NASA TN D-5198, 1969.

Hudson, W. R.; Jirberg, R. J.; and Simmons, J. H.: Flux Pinning in Superconducting Niobium Thin Films. Phys. Letters, vol. 21, no. 5, June 15, 1966, pp. 493-494.

Jirberg, Russell J.: Superconductive Dust Cores for Inductive Elements. NASA TN D-5137, 1969.

Laurence, J. C.: High-Field Magnets and Magnetic Research at NASA Lewis Research Center. Presented at the Inst. Phys. and the Phys. Soc., Oxford Univ., London, England, 1963.

Laurence, J. C.: Superconductive Magnets at Lewis Research Centre of NASA. Cryogenic Engineering: Present Status and Future Development. Heywood-Temple Ind. Publ., Ltd., 1968, pp. 94-98.

Laurence, James C.; and Coles, Willard D.: Design, Construction, and Peformance of Cryogenically Cooled and Superconducting Electromagnets. Presented at the International Symposium on Magnet Technology, Stanford, Calif., Sept. 8-10, 1965.

Laurence, J. C.; and Coles, W. D.: A Superconducting Magnetic Bottle. Advances in Cryogenic Engineering. Vol. 11. K. D. Timmerhaus, ed., Plenum Press, 1966, pp. 643-651.

Laurence, J. C.; Coles, W. D.; Brown, G. V.; and Meyn, E. H.: Performance Tests of 51-cm Bore Superconductive Magnets for a Magnetic Mirror Apparatus. Presented at Cryogenic Engineering Conference, Los Angeles, Calif., June 16-18, 1969.

Laurence, J. C.; Meyn, E. H.; and Jirberg, R. J.: Variable-Voltage, Direct-Current Power Supplies for Energizing Cryogenically Cooled and Superconductive Electromagnets. Presented at the Symposium on Engineering Problems of Fusion Research, Los Alamos, N. Mex., Apr. 8-11, 1969.

Loomis, John S.; and Hudson, Wayne R.: Low-Temperature Resistance in Minimum and Magnetoresistance for Dilute Alloys of Iron in Copper. NASA TN D-4626, 1968.

Lucas, E. J.; de Winter, T.; Laurence, J.; and Coles, W.: The Design of an 88-kG, 20-in.-Bore Superconducting Magnet System. J. Appl. Phys., vol. 39, no. 6, May 1968, p. 2641.

Papell, S. Stephen; and Faber, Otto C., Jr.: On the Influence of Nonuniform Magnetic Fields on Ferromagnetic Colloidal Sols. NASA TN D-4676, 1968.

Sass, Andrew R.: Analysis of a Distributed Superconductive Energy Converter. IEEE Trans. on Aerospace, vol. AS-2, Apr. 1964, pp. 822-825.

Sass, A. R.: Image Properties of a Superconducting Ground Plane. J. Appl. Phys., vol. 35, no. 3, pt. 1, Mar. 1964, pp. 516-521.

Sass, A. R.; and Stoll, James C.: Magnetic Field of a Finite Helical Solenoid. NASA TN D-1993, 1963.

Sarafi, Zoltan W.: Ultrasonic Attenuation in Superconducting Tantalum. NASA TN D-4806, 1968.

Sarafi, Zoltan W.; and Meyn, Erwin H.: Effect of Mechanical Vibrations on the Performance of Superconducting Magnets. NASA TN D-3954, 1967.

Schroeder, P. A.; Wolf, R.; and Woollam, J. A.: Thermopowers and Resistivities of Silver-Palladium and Copper-Nickel Alloys. Phys. Rev., vol. 138, no. 1A, Apr. 5, 1965, pp. 105-111.

Stekly, Z. J. J.; Lucas, E. J.; de Winter, T.; Strauss, B.; DiSalvo, F.; Laurence, J. C.; and Coles, W. D.: Results of Tests on Models for an 88-kG, 51-cm-Bore-Diameter Solenoid. J. Appl. Phys., vol. 39, no. 6, May 1968, pp. 2641-2646.

Woollam, J. A.: A Simple A.C. Technique for Galvanomagnetic and Shubnikov-de Haas Measurements. Cryogenics, vol. 8, Oct. 1968, pp. 312-313.

Woollam, John A.: The Nernst-Ettingshausen Effect: Predictions and Experimental Results for Metallic Tin at Low Temperatures. Bull. Am. Phys. Soc., vol. 13, no. 12, Dec. 1968, p. 1645.

Woollam, John A.: Galvanomagnetic and Thermomagnetic Effects in White Tin in Fields to 3.3 Tesla and at Temperatures between 1.2° and 4.2° K. NASA TN D-5227, 1969.

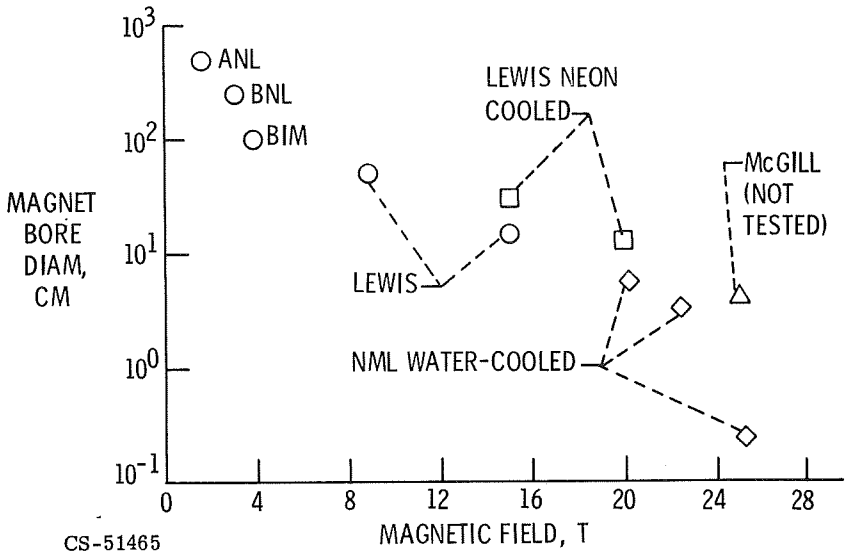

Figure V-1. - Magnet comparison.

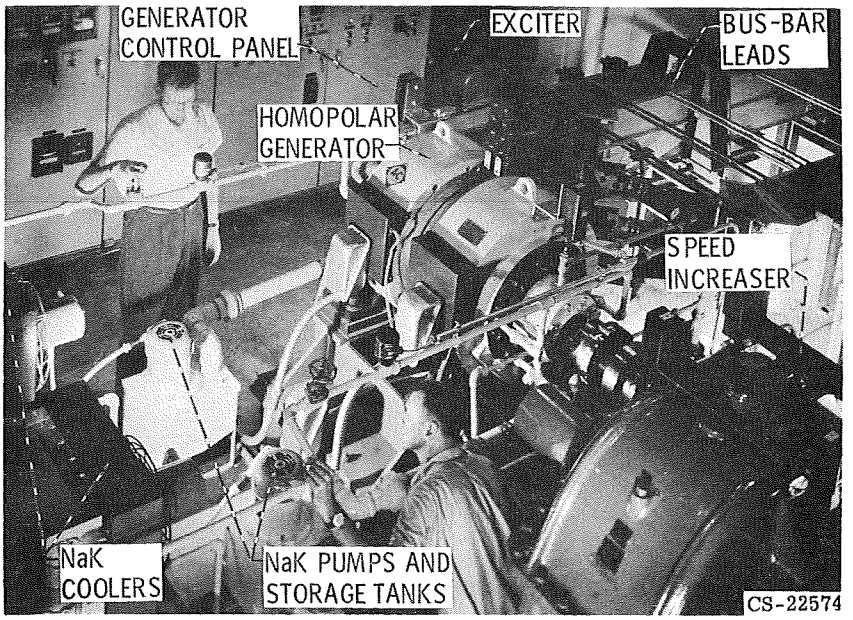

Figure V-2. - Homopolar generator installation. Drive motor off picture to right.

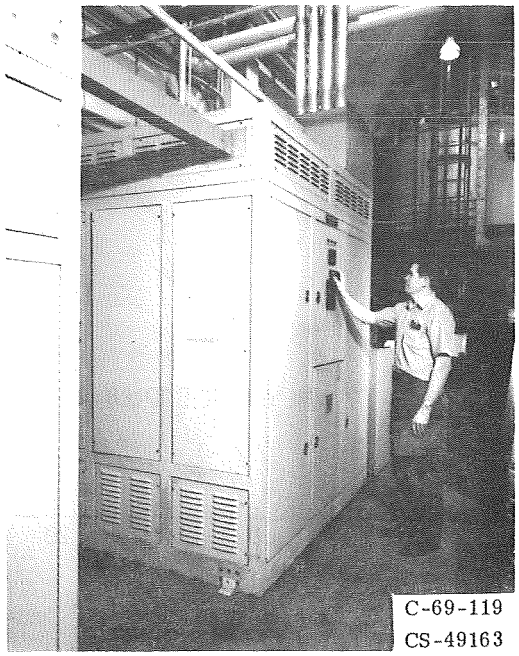

Figure V-3. - Transformer-rectifier power supply.

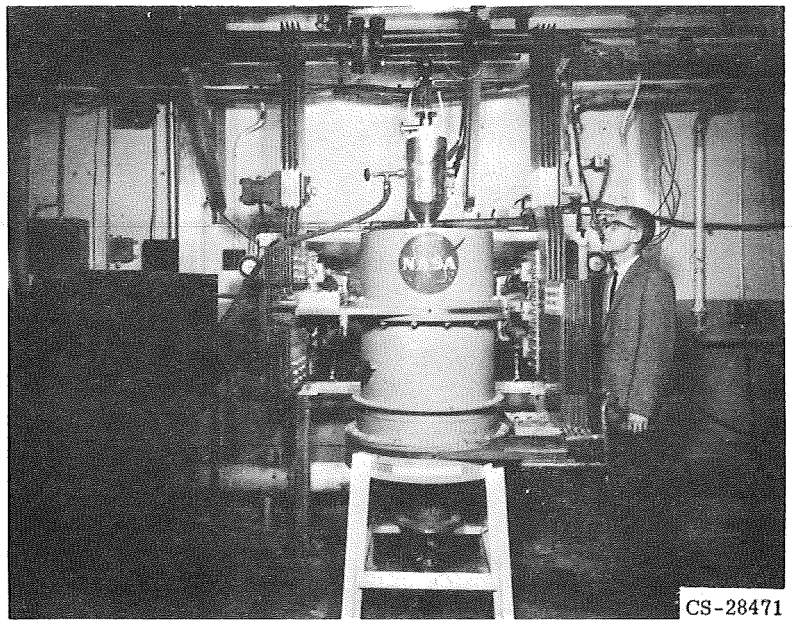

Figure V-4. - Water-cooled 8.8-tesla magnet.

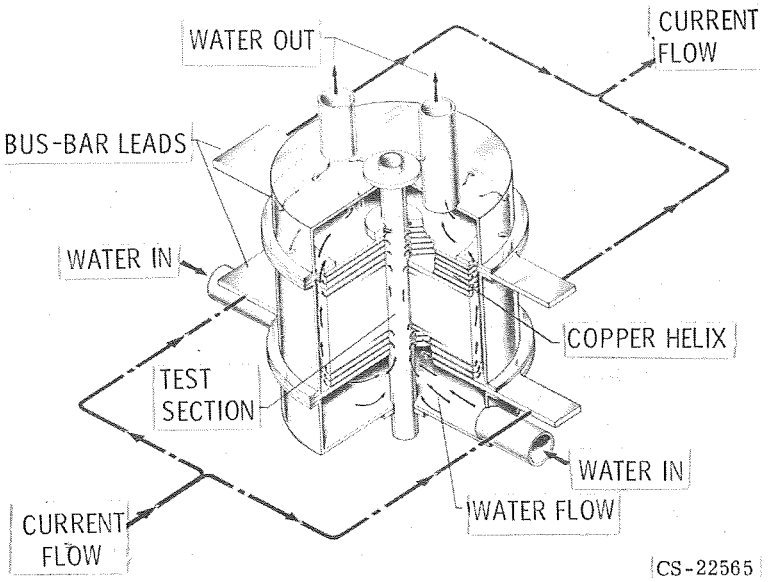

Figure V-5. - Cutaway view of water-cooled magnet.

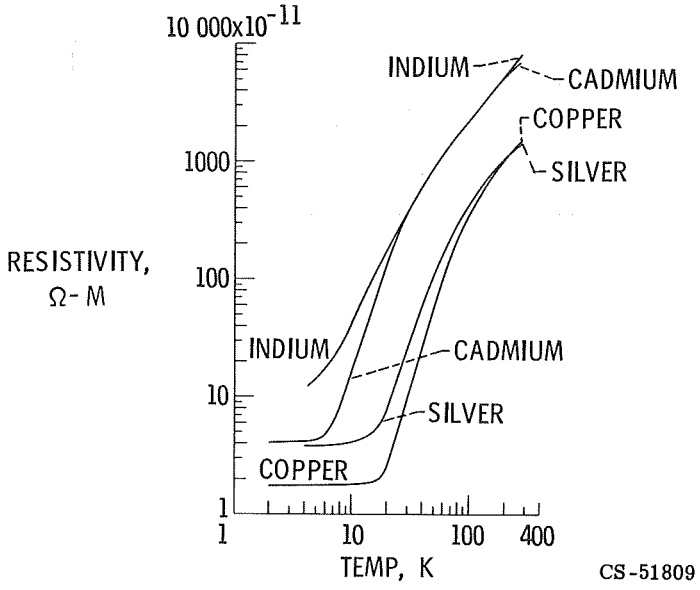

Figure V-6. - Resistivity-temperature relation for some pure metals.

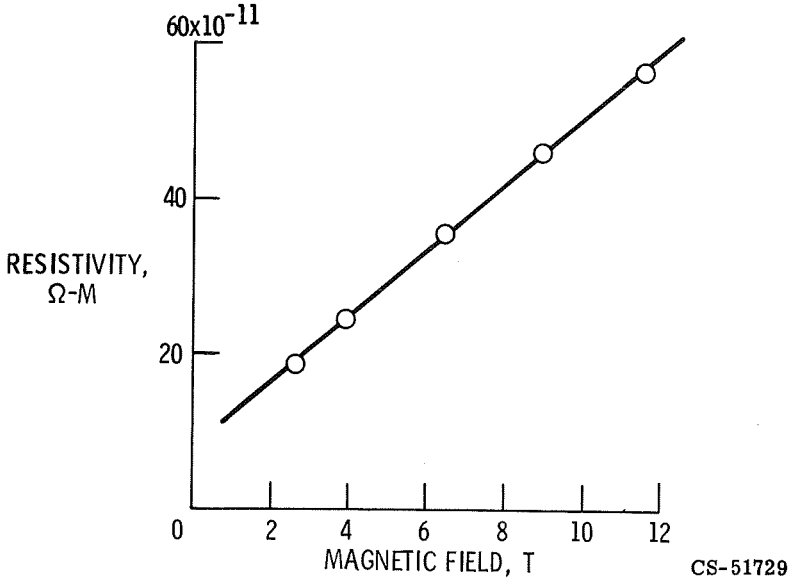

Figure V-7. - High-field magnetoresistivity of copper at 4.2 K.

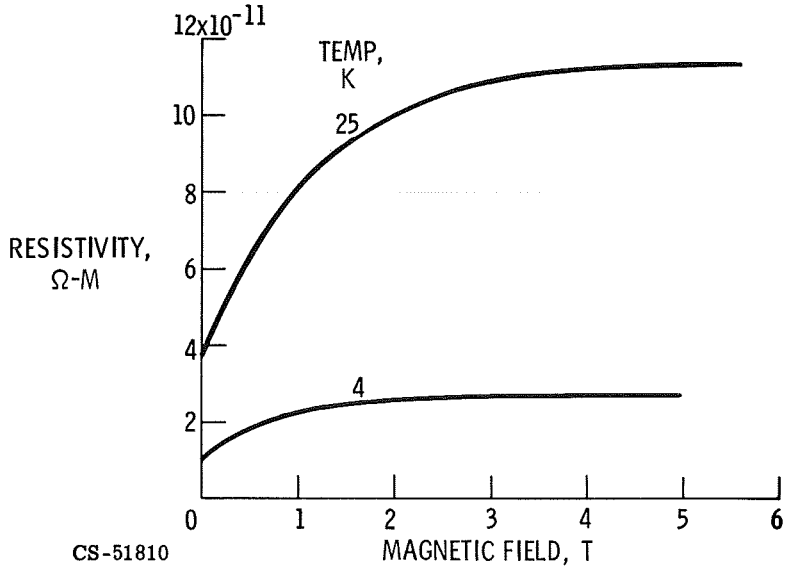

Figure V-8. - Magnetoresistivity of aluminum at two temperatures.

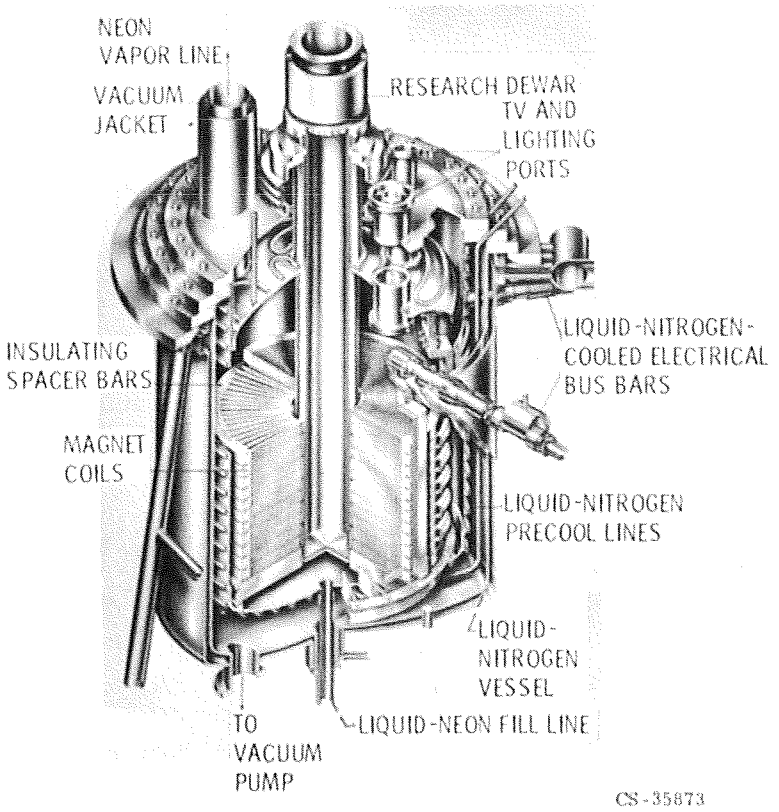

Figure V-9. - Thirty-centimeter coils in magnet vessel.

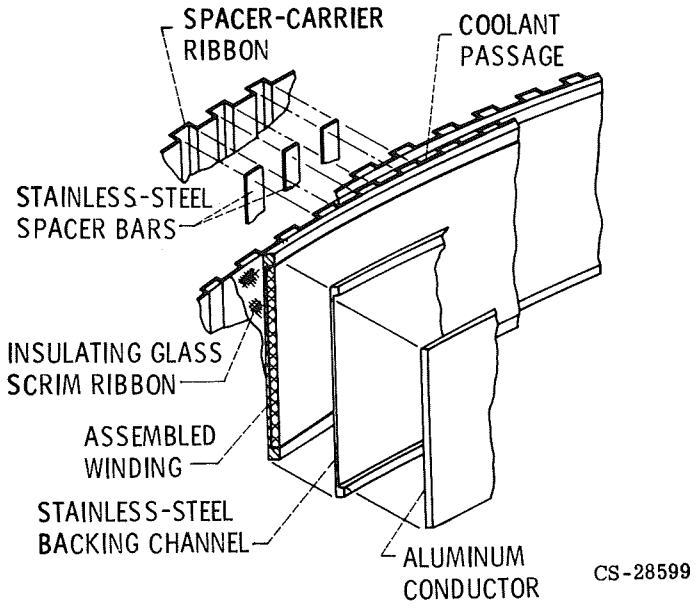

Figure V-10. - Details of coil construction.

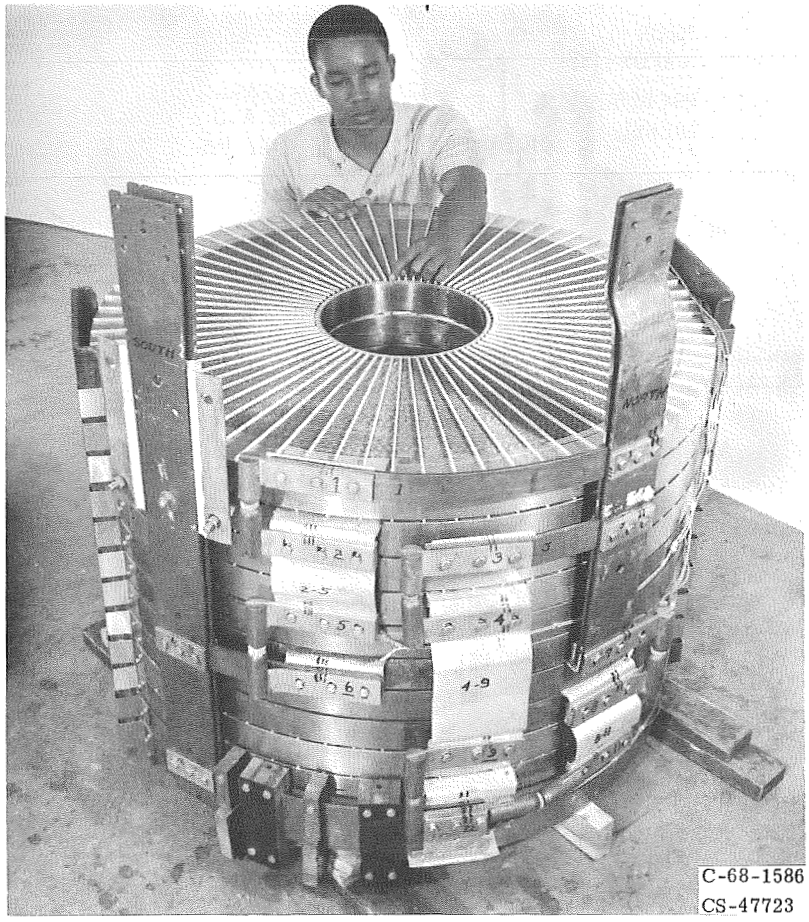

Figure V-11. - Twelve 30-centimeter-bore, liquid-neon-cooled aluminum magnet coils.

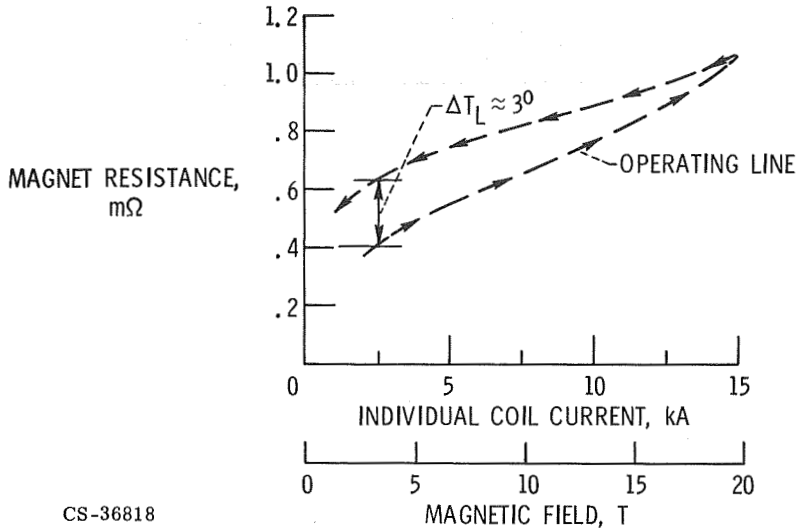

Figure V-12. - Resistance of eight coils in series-parallel for 11-centimeter-bore, 20-tesla magnet.

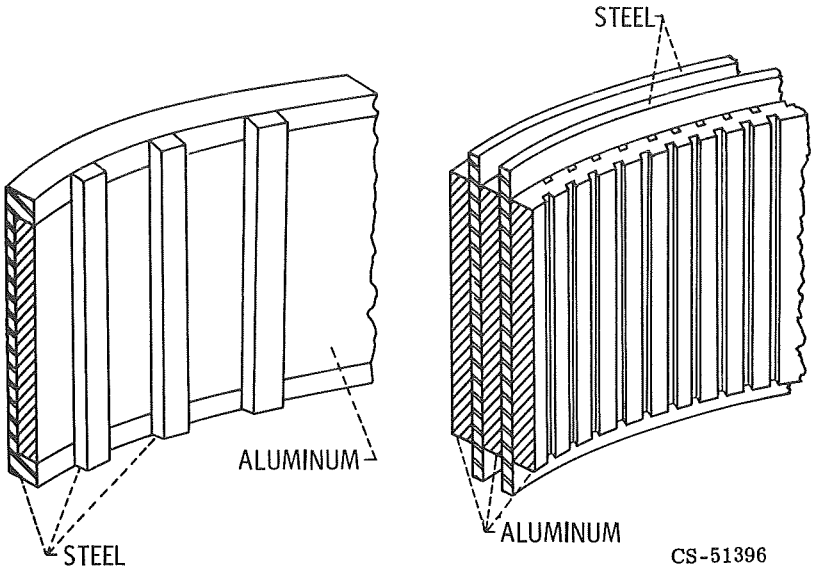

(a) Existing coil, nucleate boiling design.

(b) Proposed, nonboiling forced-convection design.

Figure V-13. - Comparison of conductors for existing cryomagnet and proposed 30-tesla design.

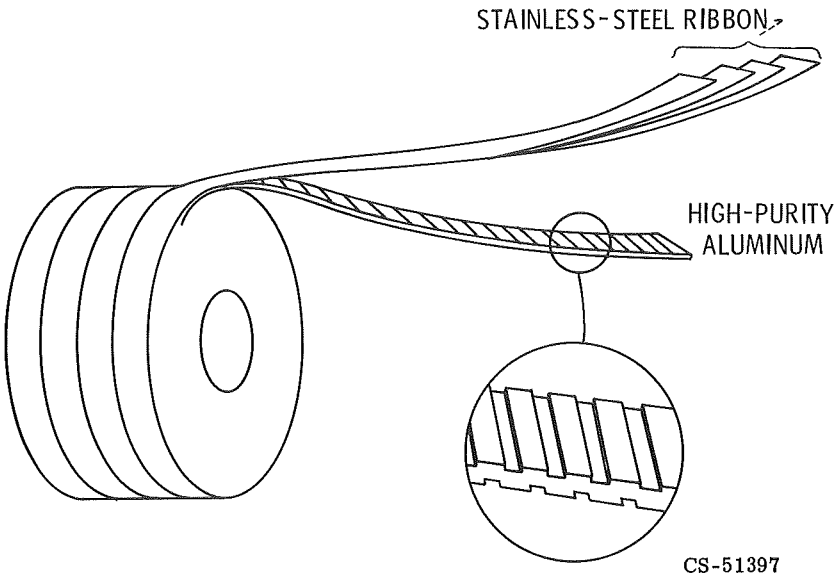

Figure V-14. - Third-generation-cryomagnet concept.

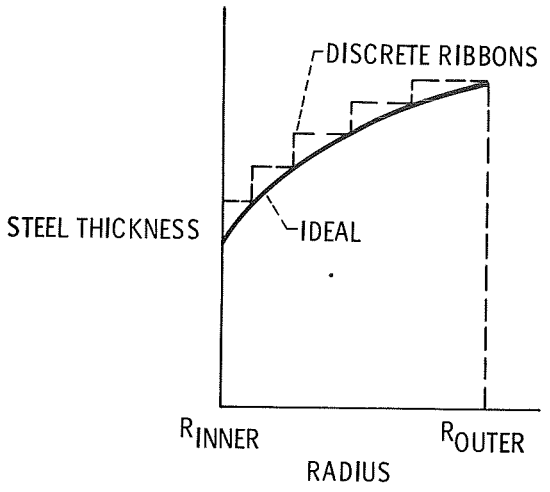

Figure V-15. - Variable structure thickness of 30-tesla coil.

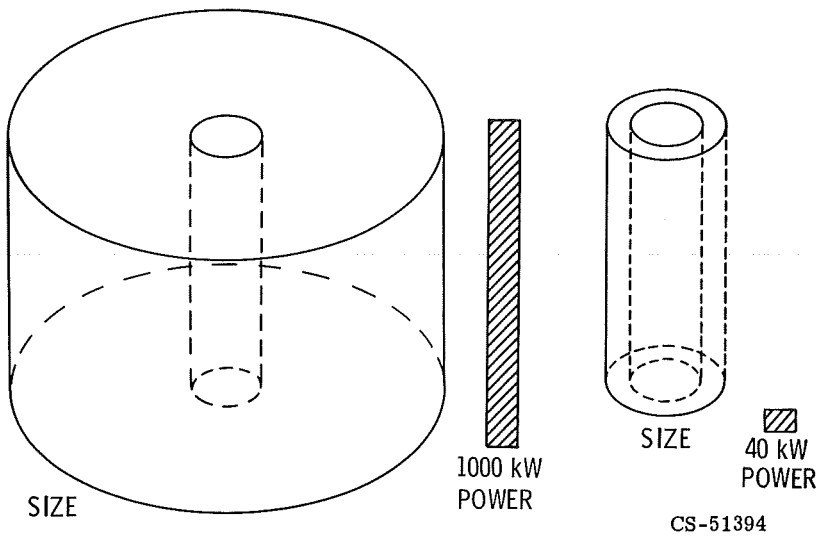

(a) Existing first-generation magnet.

(b) Third-generation concept.

Figure V-16. - Comparison of winding size and power requirement of existing 20-tesla magnet and third-generation concept.

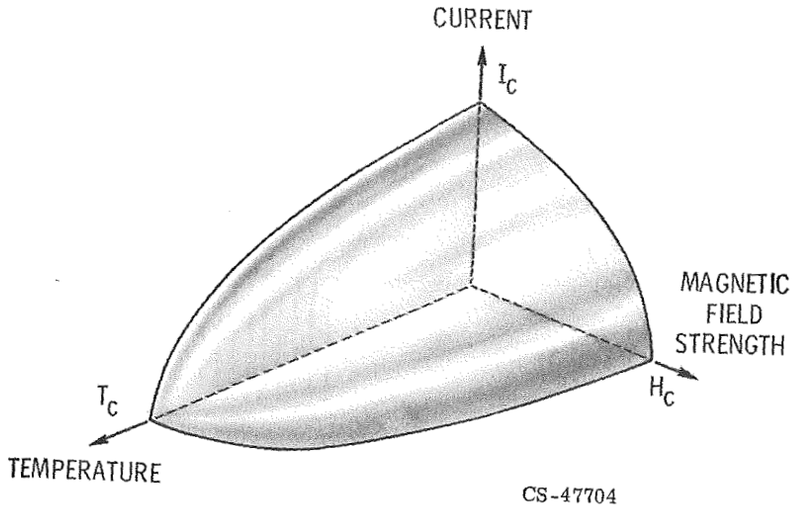

Figure V-17. - Critical surface of superconductor.

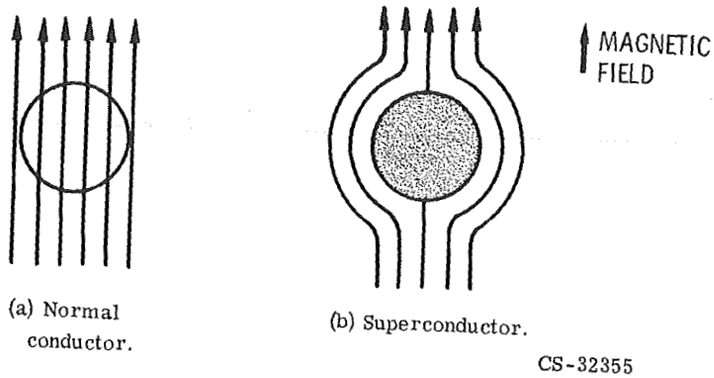

Figure V-18. - Meissner effect (magnetic field exclusion) in type I superconductor, compared with magnetic field in normal conductor.

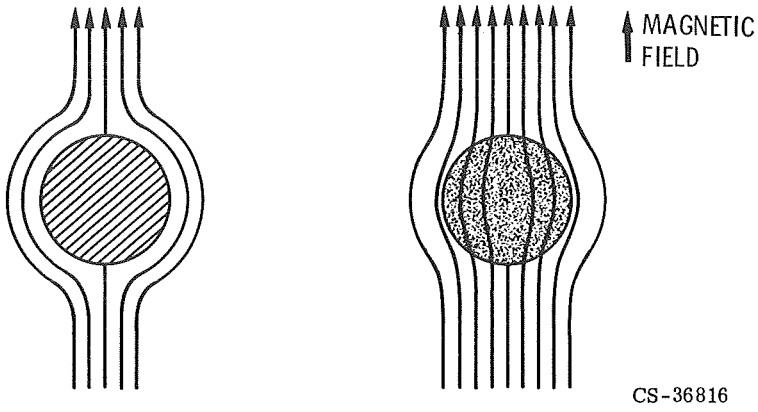

(a) At low fields (Meissner effect).

(b) At high fields.

Figure V-19. - Magnetic field behavior of high-current, high-field superconductors (type II).

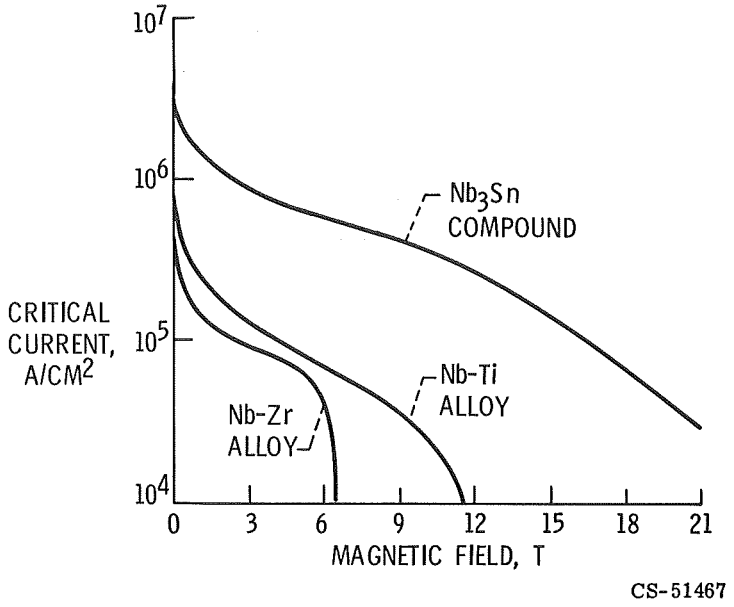

Figure V-20. - Critical current of three type II superconductors as function of magnetic field.

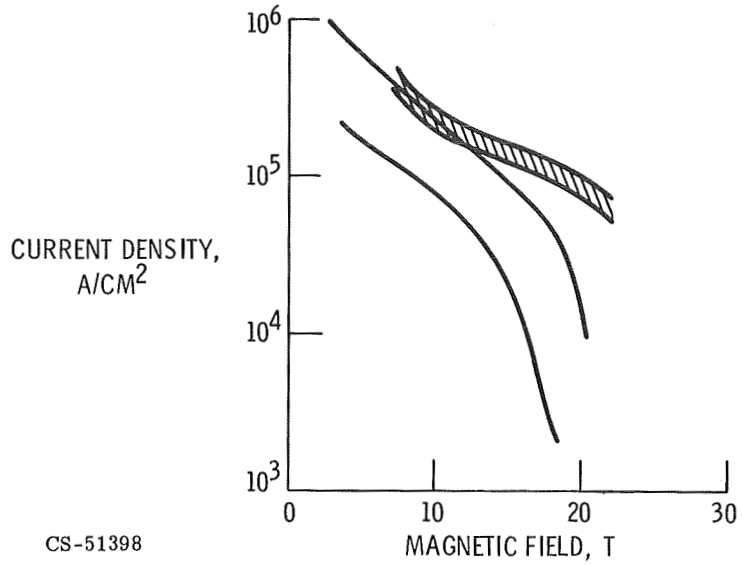

Figure V-21. - Critical current densities for Nb_3Sn produced by three different methods.

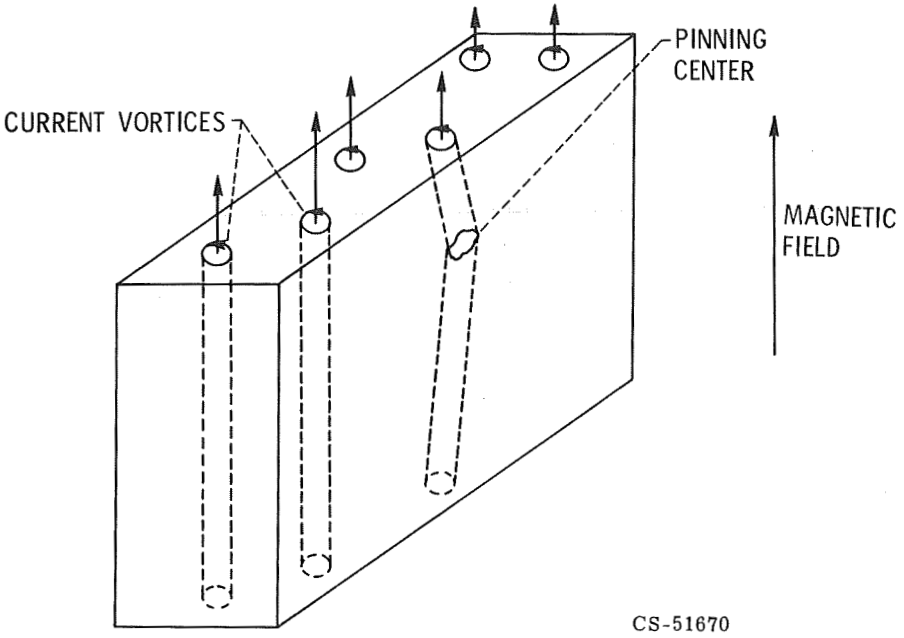

Figure V-22. - Flux lines in type II superconductors.

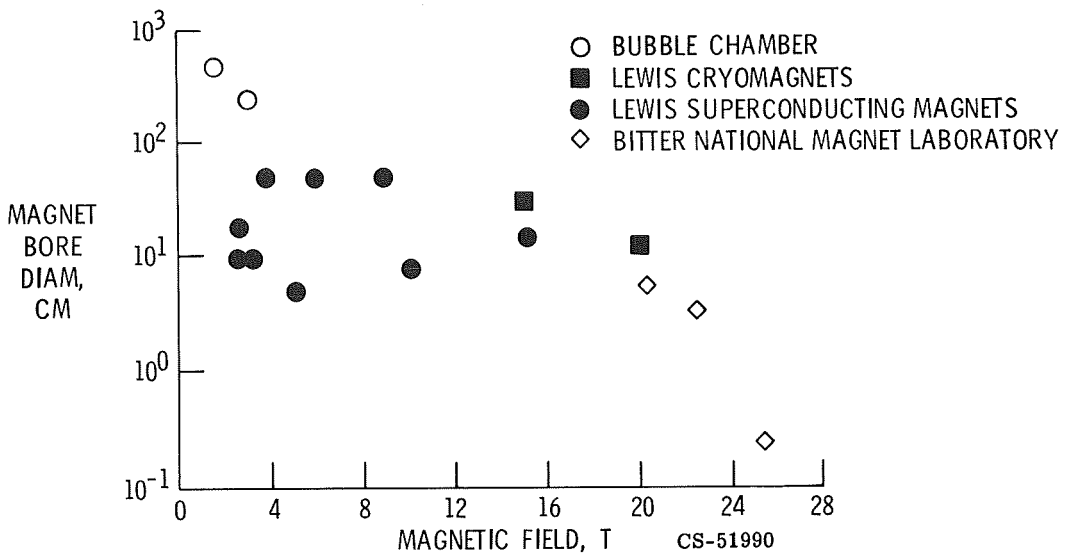

Figure V-23. - Magnet comparison.

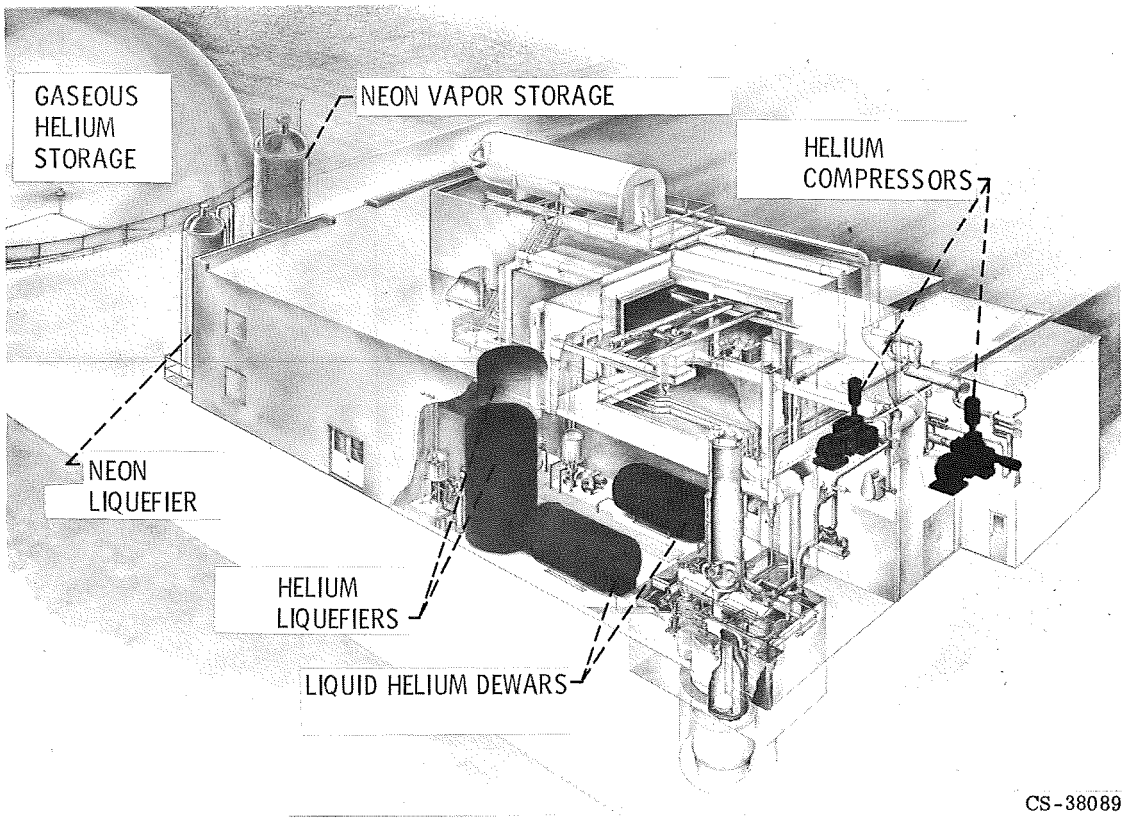

Figure V-24. - Helium reliquefaction system.

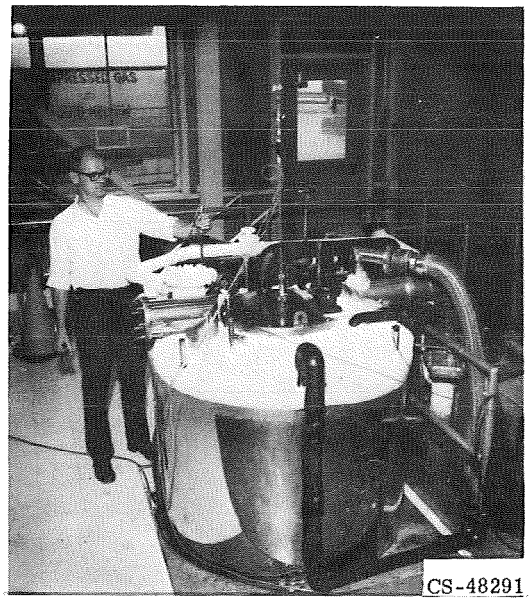

Figure V-25. - Upper section of largest magnet cryostat; inside diameter, 96.5 centimeters; height, 4.2 meters.

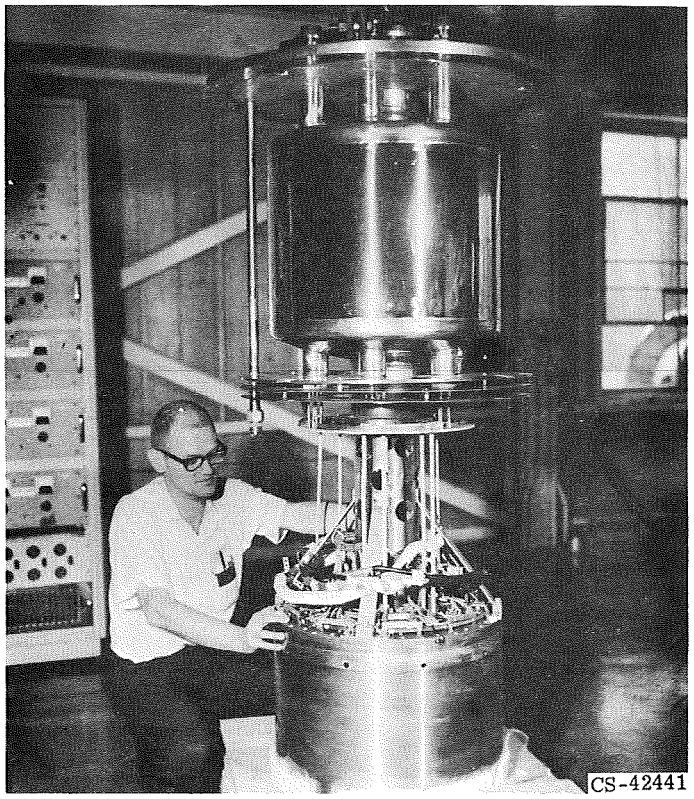

Figure V-26. - Fifteen-centimeter-bore, 15-tesla magnet and Dewar lid.

Figure V-27. - Components of magnet.

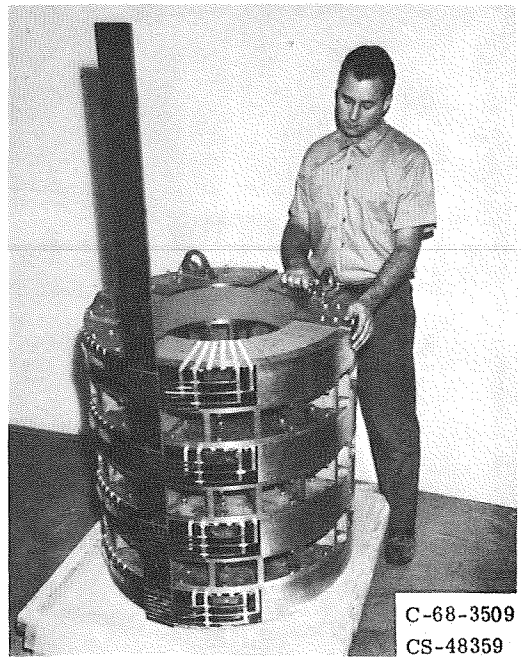

Figure V-28. - Four 51-centimeter-bore superconducting magnets.

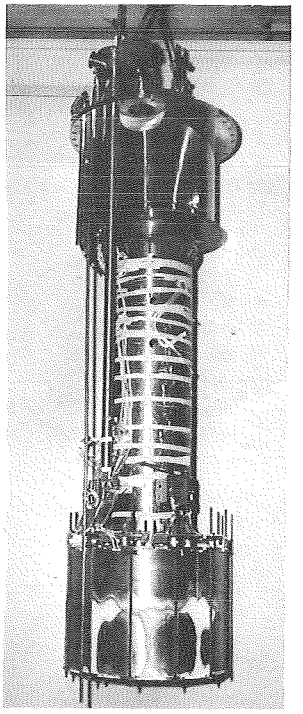

C-69-315
CS-50312

Figure V-29. - Stabilized, 51-centimeter-bore superconducting magnets mounted for testing.

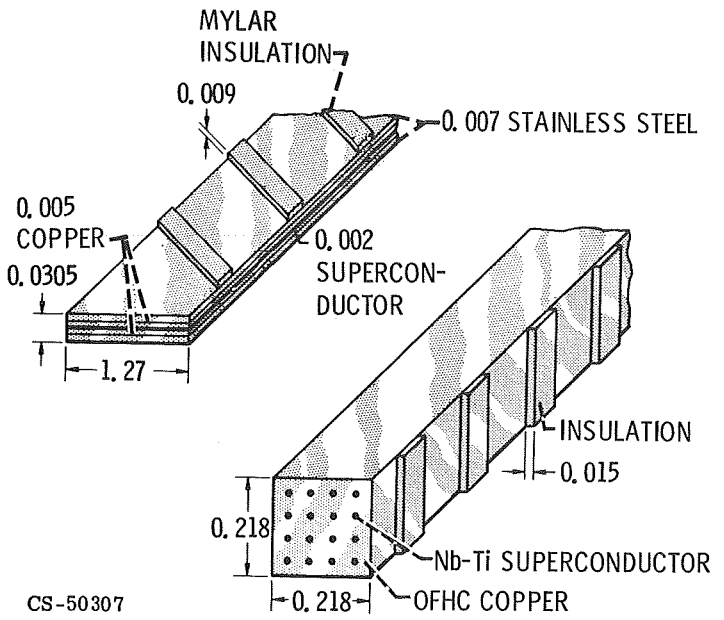

(a) Nb_3Sn conductor (stabilized).

(b) Nb-Ti conductor (stabilized).

Figure V-30. - Superconductors and insulation. (Dimensions are in cm.)

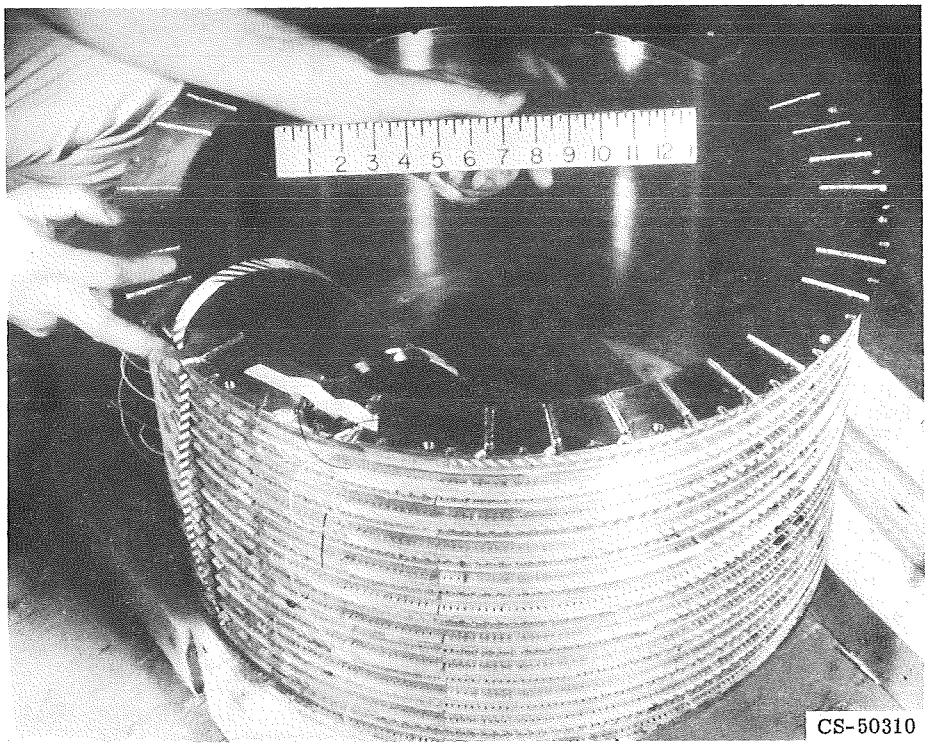

Figure V-31. - Inner module wound with Nb_3Sn tape.

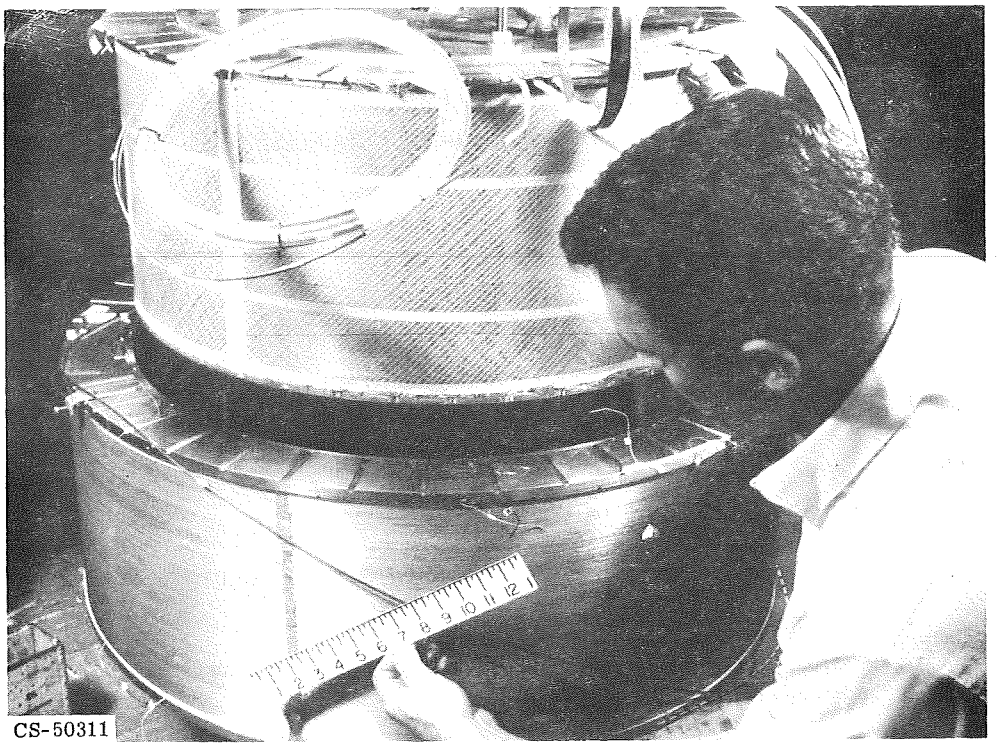

Figure V-32. - Outer and middle modules.

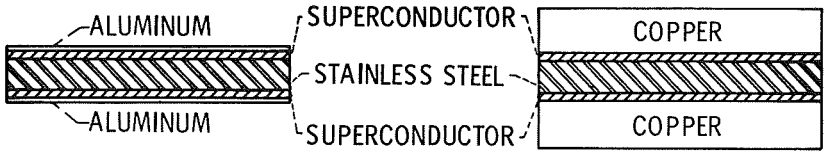

(a) Aluminum-clad conductor. (b) Copper-clad conductor.

Figure V-33. - Comparison of stabilized composites.

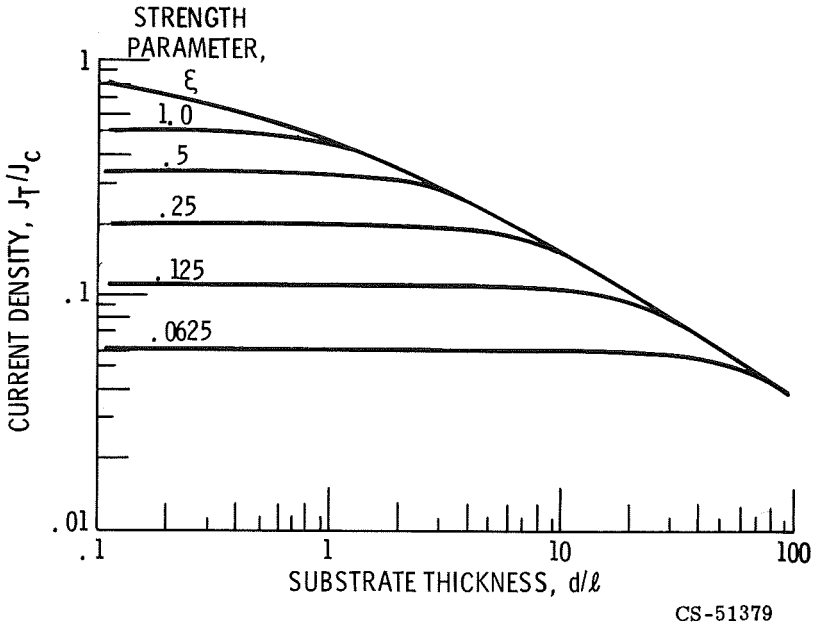

Figure V-34. - Current density as function of substrate thickness.

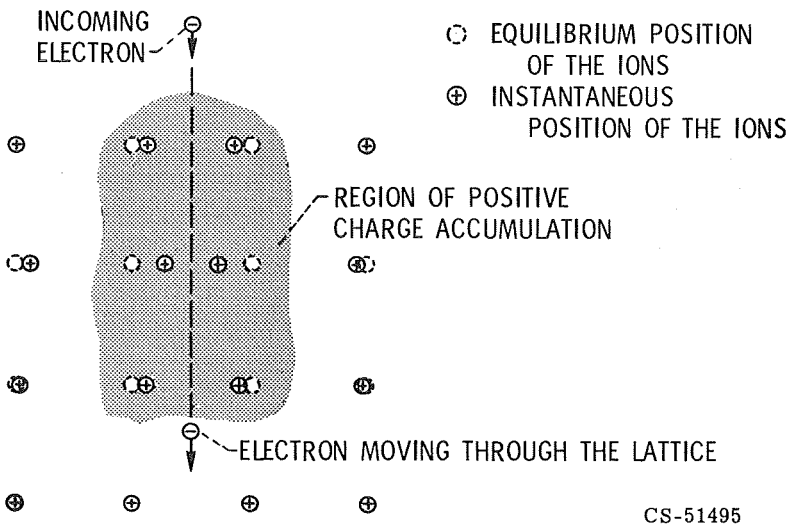

Figure V-35. - Electron-phonon interaction.

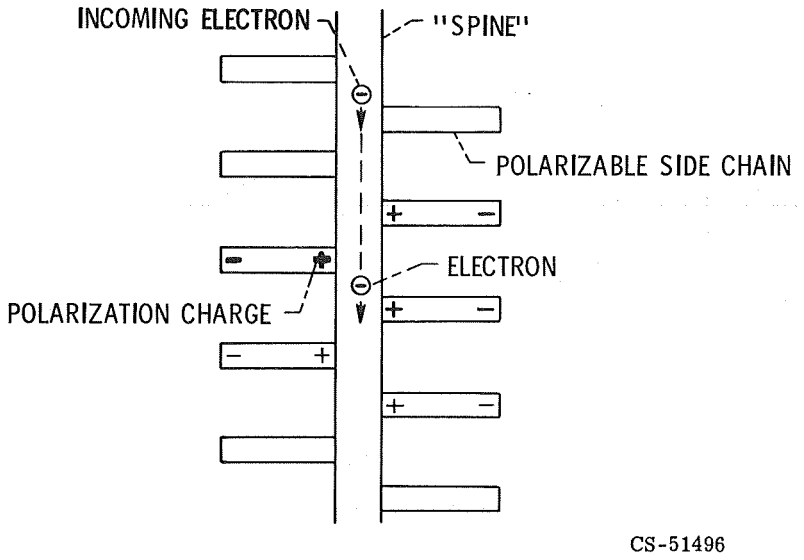

Figure V-36. - Superconductive organic molecule.

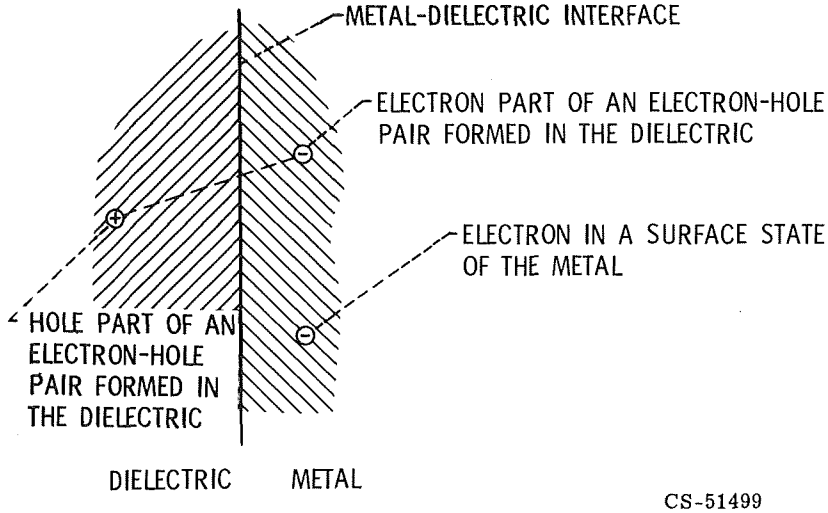

Figure V-37. - Excitonic superconductor.